



HAL
open science

Local activation of light-induced degradation in co-doped boron-phosphorus silicon: Evidence of defect diffusion phenomena

M. Najjar, B. Dridi Rezgui, M. Bouaicha, O. Palais, B. Bessais, S. Aouida

► To cite this version:

M. Najjar, B. Dridi Rezgui, M. Bouaicha, O. Palais, B. Bessais, et al.. Local activation of light-induced degradation in co-doped boron-phosphorus silicon: Evidence of defect diffusion phenomena. *Materials Science in Semiconductor Processing*, 2021, 135, pp.106104. 10.1016/j.mssp.2021.106104 . hal-03512883

HAL Id: hal-03512883

<https://amu.hal.science/hal-03512883v1>

Submitted on 7 Mar 2022

HAL is a multi-disciplinary open access archive for the deposit and dissemination of scientific research documents, whether they are published or not. The documents may come from teaching and research institutions in France or abroad, or from public or private research centers.

L'archive ouverte pluridisciplinaire **HAL**, est destinée au dépôt et à la diffusion de documents scientifiques de niveau recherche, publiés ou non, émanant des établissements d'enseignement et de recherche français ou étrangers, des laboratoires publics ou privés.

Local activation of light-induced degradation in co-doped boron-phosphorus silicon: evidence of defect diffusion phenomena

M. Najjar^{1,2}, B. Dridi Rezgui¹, M. Bouaicha¹, O. Palais³, B. Bessais¹, S. Aouida¹

¹Laboratoire de Photovoltaïque, Centre de Recherches et des Technologies de l'Énergie, Technopôle de Borj-Cédria, Hammam-Lif, 2050, BP 95, Tunis, Tunisie

²University of Tunis, Higher National Engineering School of Tunis (ENSIT), Tunis, Tunisia, 1008

³Aix Marseille Université, Université de Toulon, CNRS, IM2NP, 13397, Marseille, France

Corresponding author: salma.aouida@crten.rnrt.tn;

Abstract:

In this study, we are interested in the local activation of Light-induced degradation (LID) defect in highly co-doped silicon wafers with boron and phosphorus. For this purpose, the experiments were focused on measuring the minority carrier lifetime before and after LID activation via a mapping technique. It has been found that the LID defect density exhibits a Gaussian distribution centered on the excitation point of the laser beam; the intensity of the Gaussian distribution of the LID defect varies with the concentration of the co-dopants. The lifetime of the minority carriers was found to decrease in all regions of the silicon sample while the excitation laser beam was focused on an area of approximately 1 mm². This indicates that LID defects are activated even in unexcited regions of silicon wafers, suggesting a LID diffusion phenomenon from the laser excitation point to the whole silicon wafer. It was demonstrated that high phosphorus doping-level in silicon wafers leads to a significant reduction in the LID effect.

1. Introduction

Light-induced degradation (LID) has received considerable attention in recent years due to its detrimental impact on the performance of photovoltaic (PV) solar cells under field conditions [1]. Several studies investigating this effect have been published and introduced various trends and interpretations [2-15]. LID phenomenon was firstly presented in 1973 by Fischer and Pschunder [2]; they observed a significant degradation of the efficiency of Cz-based silicon solar cells under illumination. This degradation stops after a few hours of illumination and is eliminated after a heat treatment at a low temperature around 200 °C [2]. Measurements of the decrease in photoconductance have shown that the observed degradation is due to a decrease in the lifetime of minority carriers of the solar cell base material. It was suggested that the minority carrier lifetime balances between two levels: high and low values after low-temperature treatment and illumination, respectively [2, 5]. The carrier lifetime variation was attributed to the activation/annihilation of electrically active defects. Since this observation, various models and interpretations have been proposed to explain the origin of these defects. Later in 1979 Weizer et al. [16], reported photo-degradation in n⁺/p silicon solar cells under illumination at open circuit operation, and under illumination with specific wavelength at short circuit operation [16]. The spectral response of the cells shows that the recombination centers (responsible for the minority carrier decrease) are located in the base (p-type region) region of the solar cell and not in the diffused region (n⁺-type region) [16]. In a first interpretation, Weizer et al. associated the activated recombination centers with defect pairs formed by a lattice defect and silver atom or complex of atoms introduced in the cell-contact metallization step. This assumption is weak because the minority carrier lifetime decreases also under illumination in passivated silicon wafer. Corbett et al. [17], indicated that various types of defect-pairs could be activated in an illuminated boron-doped silicon wafer; they reported more than 50 possible reactions for defect formation. Several years later Knobloch et al. [3] reported that the

degradation in boron-doped silicon is caused by the presence of excess minority carriers and not photons. This result was confirmed by Glunz et al. [18] and Hashigami et al. [7]. The more esteemed origin of LID in silicon is attributed to B-O defects and was discovered and electrically identified by Schmidt et al. [4, 19]; they showed that the LID phenomenon depends on boron concentration while it is absent in gallium-doped and Fz-boron-doped silicon wafers. The study of the kinetic formation of LID – related defects or more explicitly B-O complexes reveals the appearance of two degradation mechanisms [6, 20-22]. For typical p-type silicon wafers, degradation occurs via a rapid initial decrease in minority carrier lifetime through rapidly fast-forming recombination centers (FRCs) within minutes, followed by slower decay on a timescale of several tens of hours to a few days due to slow-forming recombination centers (SRC). Most studies on p-type silicon show that the influence of the SRC on the device operation of the solar cell is stronger than for the FRC. Therefore, the problematic degradation focuses mostly on SRC, while the influence of FRC is often neglected. Schmidt et al. [5] introduced a model where the defect is formed by the fast diffusion of oxygen dimer (positively charged) that capture the immobile substitutional boron atoms (negatively charged) to form B_s-O_2 recombination centers; in such a situation the concentration of the metastable boron-oxygen complex in crystalline silicon depends proportionally on the substitutional boron concentration and in a quadratic manner on the interstitial oxygen content. This model was prevailing for many years but was invalidated by Macdonald et al. [23] when they discovered that the degradation is controlled by the concentration of holes $[p_0]$ rather than the concentration of boron $[B]$. In 2010, Voronkov and Falster [24] proposed a new degradation model in which degradation starts from a latent complex B_iO_2 formed by an interstitial boron atom and an oxygen dimer. After carrier generation, a reconstruction of B-O complexes results in the production of recombination centers. This model is the first one that demonstrates the proportionality between defects concentration and holes concentration $[p_0]$ in boron-

phosphorus co-doped silicon. However, recent work carried out in 2016 [25] has shown that the two latent B-O₂ defects (the precursors of FRC and SRC) are created during the cooling step of the silicon ingot, and their concentration is proportional to the boron concentration [B_i⁺] and the squared oxygen concentration [O_{2i}]. Today, no model can fully explain all experimentally observed characteristics associated with the defect responsible for light-induced degradation and it is still possible to draw some conclusions on the nature of the defect.

Besides, most previous works were focused on p-doped silicon (exclusively) with boron, while recently the LID has been studied in both boron (p-type) and phosphorus (n-type) Cz-Si [26]. Results based on compensated p-type Cz-Si show that the compensation reduces the recombination strength of BO_{2i} complexes and their concentration depends on the net doping, (i.e., [B]-[P]). B atoms and P atoms form BP pairs [9, 23, 27], which minimizes the defect concentration since all Boron may be compensated. Thus, the B-P-compensated n-Si can be affected by the LID, i.e. some BO_{2i} are formed, but their recombination activity is weaker than in p-Si, due to asymmetric electron and hole capture cross-sections.

In this work, we focus on compensated silicon wafers co-doped with boron and phosphorus. We examine the effect of the net-doping on the minority carrier lifetime and the activation of LID defect. Minority carrier lifetime mapping before and after sample illumination enables to estimate of the LID defect density. Mapping investigations show a Gaussian distribution of the LID defect density centered on the excitation point. The defect density decreases with the increase of phosphorus amount. As far as we know, it is the first time that a mapping of the LID defect density was reported, showing that LID defect diffuse through the sample. The LID defect diffusion process may be the origin of the observed slow defect generation.

2. Experiments

This study was carried out on highly doped silicon samples cut from wafers originating from the same monocrystalline Czochralski silicon (Cz-Si) ingot intentionally doped with boron (B)

and phosphorus (P) atoms. During the crystallization step, the dopant impurities were progressively incorporated in the melt of the silicon bath. Their various segregation coefficients lead to very wide resistivity values along the ingot [28, 29]. Depending on the wafer position in the formed ingot, intrinsic, p-type, and n-type crystalline silicon wafers are formed. The concentrations of boron and phosphorus were determined by Glow-Discharge Mass Spectroscopy (GDMS) measurements [30, 31]. The resistivity was measured with a four-probe system. Table 1 summarizes the properties of the studied samples. The interstitial oxygen concentration obtained by Fourier transformed infrared (FTIR) measurements is around $8.5 \cdot 10^{17} \text{cm}^{-3}$. The samples were double-sides passivated by hydrogenated silicon nitride ($\text{SiN}_x\text{:H}$) coat using a plasma-enhanced-chemical-vapor-deposition (PECVD) process to minimize surface recombination. A $200^\circ \text{C}/60 \text{ min}$ dark annealing in a furnace tube quartz was used to annihilate the LID complexes and to reach the initial annealed state before light treatment [12]. Effective lifetime measurements and mapping investigations were done using $\mu\text{PCD WT2000-VPN}$ from Semilab with $250 \mu\text{m}$ scan resolution. A lifetime mapping was performed on each sample before and after light treatment. The local defect activation was carried out using a pulsed laser excitation with a wavelength of 904 nm and a spotlight of 1 mm^2 . The penetration depth of this wavelength in silicon is about $30 \mu\text{m}$. Simultaneously, the effective carrier lifetime (τ_{eff}) was measured using $\mu\text{PCD Semilab WT2000-VPN}$ equipment. To eliminate the edge effect, we focus mapping investigations on a circle centered in the excitation point with a diameter of 20 mm . We suppose that the activated defects are the well-known boron oxygen-related light-induced degradation (BO-LID) complex [32].

3. Results and discussion

3.1 Effect of phosphorus compensation on minority carrier lifetime of boron-doped silicon wafers

Co-doping silicon wafer by boron and phosphorus reduces the majority carrier concentration, which could be expressed by the co-doping amount or the net doping $p_0 = [B] - [P]$ for p-type doping and $n_0 = [N] - [B]$ for n-type doping.

	[B] (10^{17} cm^{-3})	[P] (10^{17} cm^{-3})	$P_0 = [B] - [P]$ (10^{17} cm^{-3})	Resistivity ($\Omega \cdot \text{cm}$)	Average of initial τ_{eff} (μs)
Sample A	2.80	1.60	1.20	0.35	2.3
Sample B	3.00	1.85	1.15	0.51	12
Sample E	4.15	5.30	-1.20	0.61	32

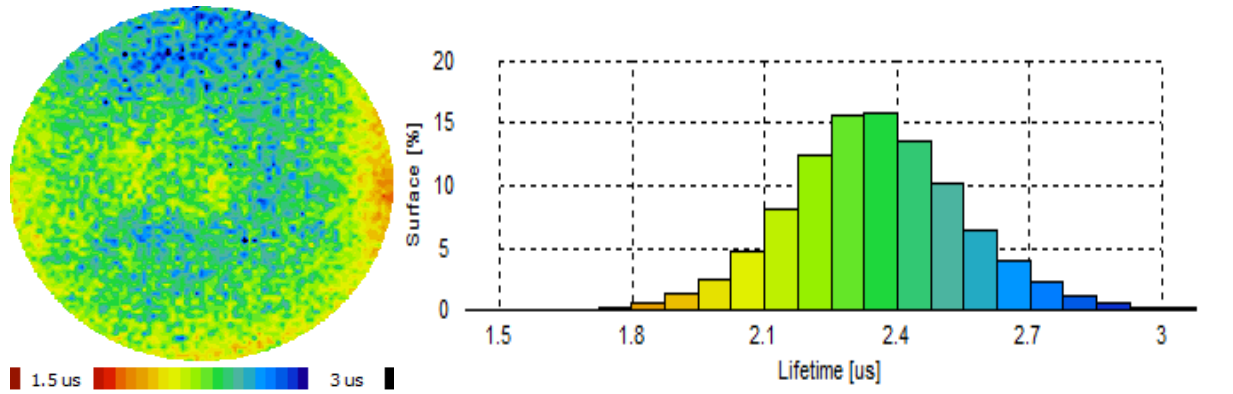
Table 1: Doping levels, resistivity, and average effective lifetime values of studied samples.

Table 1 presents the average of the initial lifetime, before LID activation, of the studied samples and their net doping values. It is worth noting that samples studied in this work were taken from different height positions of the ingot and are labeled A, B (p-type doped), and E (n-type doped). For sample A, where p_0 is about $1.2 \times 10^{17} \text{ cm}^{-3}$, the average lifetime value is $2.3 \mu\text{s}$. This value increases to $12 \mu\text{s}$ for sample B where p_0 is equal to $1.15 \times 10^{17} \text{ cm}^{-3}$. The compensation induces an improvement in the value of the initial lifetime values, as shown in previous work [26]. This is explained by the compensation-induced reduction of the recombination strength of shallow energy levels as well as the Auger and radiative recombination rates [31]. In fact, minority carrier lifetime illustrates the average time that the carrier remains free after its generation. This parameter depends on the carrier recombination process and gives valuable information about the low defect densities [33]. For surface-passivated silicon samples, like the studied ones, the main process is associated with bulk Shockley-Read-Hall (SRH) recombination mode [33, 34]. This model is governed by traps having energy levels (E_t) in the forbidden band. Generally, these traps are associated with doping species, metal impurities, and crystal defects. Boron is an acceptor element, that gives rise to a shallow level in the vicinity of the valence band having

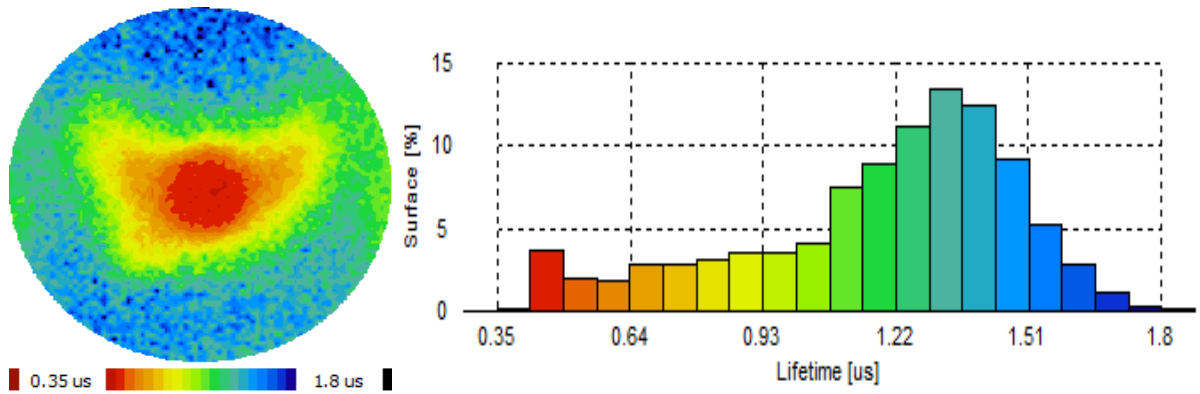
an energy of about $E_A - E_V = 0.045$ eV [35]. The recombination occurs through excess holes in the valence band [33]. The strength of this process is sensitive to carrier concentration (i.e. doping amount). Highly doped materials ($>10^{17}$ cm⁻³) present low lifetimes [36]. The decrease of the majority carrier concentration increases the minority carrier lifetime. Phosphorus is a donor element giving a shallow level in the vicinity of the conduction band having an energy $E_C - E_D = 0.045$ eV [35]. The co-doping reduces the excess holes by the formation of BP pairs in p-type samples which explain the difference of the average of initial lifetime values between samples A and B (Table 1). For sample E the average lifetime increases to 32 μ s this is explained by the fact that holes became the minority carriers.

3.2 Local LID defects activation

LID defects in silicon samples can be activated through light exposure [2, 23]. The local LID is activated via a pulsed laser excitation having a wavelength of 904 nm ($12 \cdot 10^{12}$ photons/pulse) and a spotlight having a surface area of 1 mm². Figure 1-a presents the lifetime mapping and the surface histogram of the sample (A) after a total annihilation of LID defects by dark thermal treatment at 200 °C for 60 min. The lifetime exhibits a Gaussian distribution in the 1.5 μ s - 3 μ s range with an average value of 2.3 μ s. Figure 1-b shows the lifetime mapping and the surface histogram of sample (A) after local LID activation during 20 hours; this process leads to a total activation of LID defects at the excitation focal point. It is worth noting the existence of two regions. The first one corresponds to the center of the excitation point (LID-spot) and is associated with very low lifetime values between 0.35 μ s and 0.6 μ s. The second region, which is outside the excitation spot, corresponds to lifetime values of about 1.8 μ s, lesser than the initial average lifetime value (2.3 μ s). This interesting result suggests that the LID defect diffuses throughout the whole silicon sample.



(a)



(b)

Fig. 1 Mapping and histogram minority carrier lifetime of sample A: (a) de-activation of LID defect after dark thermal treatment at 200 °C during 60 min (average lifetime = 2.3 μ s), (b) after local LID activation (average lifetime = 1.3 μ s)

To quantify the spatial distribution of LID defect we convert lifetime mapping into the effective LID defects concentration (N^*) mapping [37]; N^* is defined as $1/\tau_{fm} - 1/\tau_{im}$, where τ_{im} and τ_{fm} are the initial and the final measured lifetime considered in the same sample position, respectively. Figure 2 depicts the corresponding mapping, the surface histogram, and the diametric line scan.

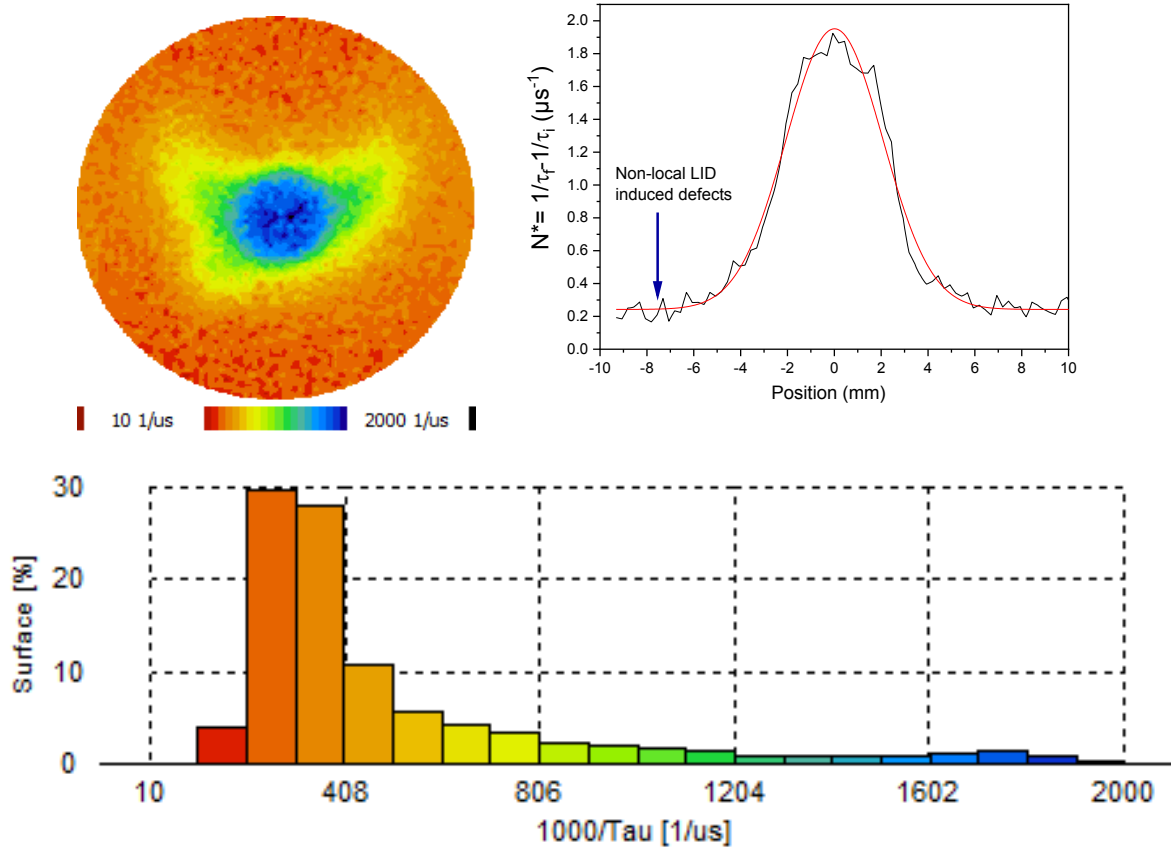


Fig. 2 Mapping, histogram, and a line scan of effective LID defects concentration N^* of sample A

LID defect concentration goes along a Gaussian distribution having a Full Width at Half Maximum (FWHM) of 4.8 mm and centered in the excitation point where N^* is about $1.9 \mu\text{s}^{-1}$. Diffused defects labeled non-local LID defects diffuse throughout the silicon sample; for sample (A) they reach a concentration of $0.2 \mu\text{s}^{-1}$ far away from the excitation point (Fig. 2). These values of LID defect density are relatively high as compared with other studies [23], this is due to the fact high doping level of the silicon samples (10^{17}cm^{-3}) that leads to amplification of light effect.

3.3 Effect of phosphorus compensation on local LID activation

The same treatment and analysis were carried out on samples B and E; their corresponding mapping, surface histogram, and diametric line scan of LID defects concentration are shown in figures 3 and 4. The main properties of the formed LID defects in all samples are summarized

in table 2. We notice that as p_0 decreases from $1.2 \cdot 10^{17} \text{ cm}^{-3}$ (sample A) to $1.15 \cdot 10^{17} \text{ cm}^{-3}$ (sample B) the effective concentration (N^*) of the local defect moves from $1.9 \mu\text{s}^{-1}$ to $0.7 \mu\text{s}^{-1}$ indicating a decrease in LID defect activation; in this case, the effective concentration of non-local defects decreases from $0.2 \mu\text{s}^{-1}$ to $0.04 \mu\text{s}^{-1}$, and the LID-spot slightly decreases from 4.7 mm to 4 mm (Table 2). The increase in P concentration (sample B) corresponds to a decrease in hole concentration, which is the result of a low LID defect activation.

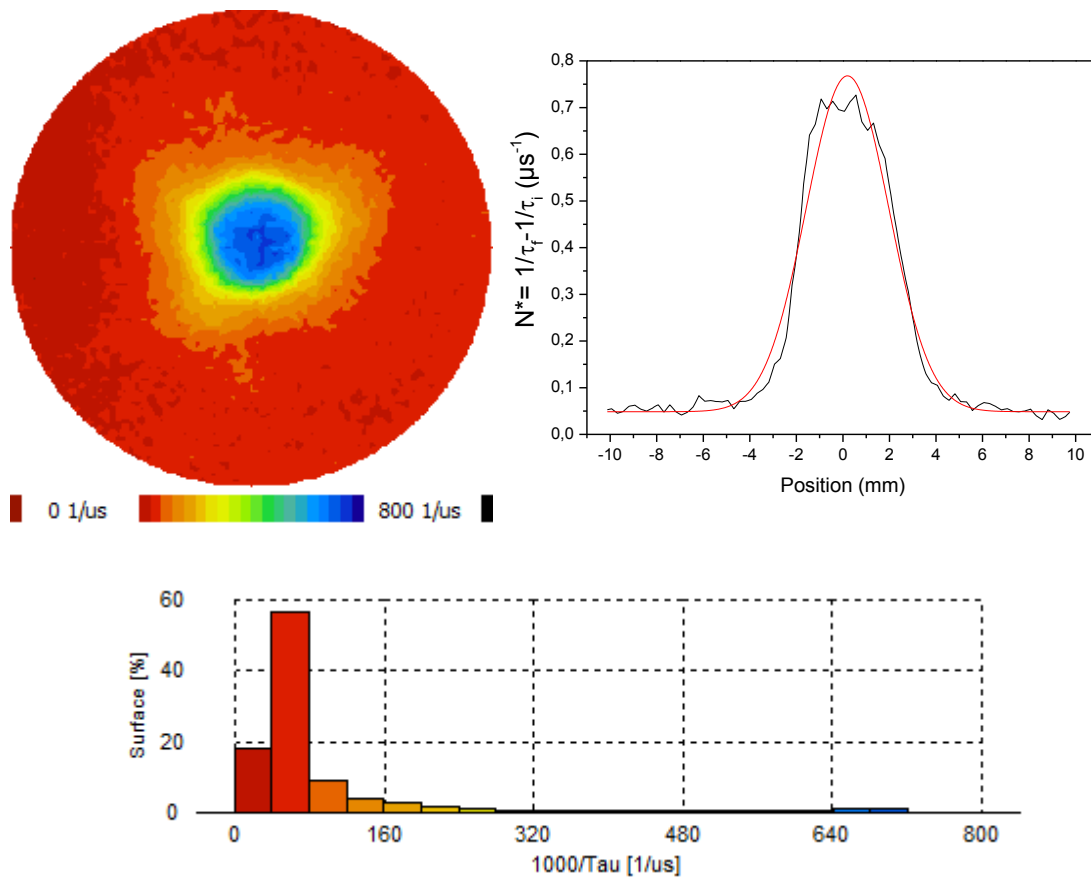


Fig. 3 Mapping, histogram, and a line scan of effective LID defects concentration N^* of sample B

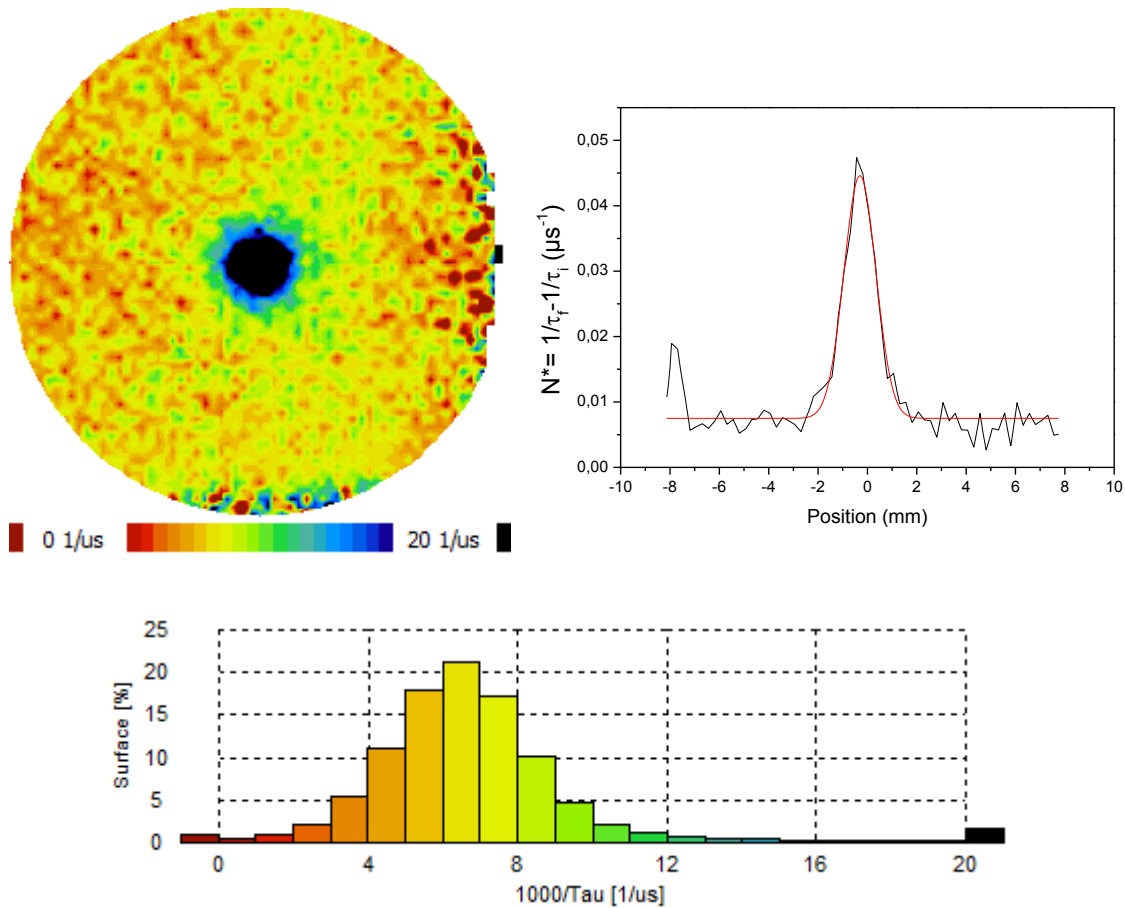


Fig. 4 Mapping, histogram, and a line scan of effective LID defects concentration N^* of sample E

It is interesting to note that for the n-type co-doped silicon sample (Sample E), the local LID defect concentration value is about $0.045 \mu\text{s}^{-1}$, LID activation is rather weak, the diffused non-local LID defects can be neglected (around $0.007 \mu\text{s}^{-1}$) and the LID-spot is around 1.5 mm, quasi-equal to that of the laser spot. It is important to remember that in sample E the boron concentration is $4.15 \cdot 10^{17} \text{ cm}^{-3}$, higher than that of samples A and B (Table 1). This result perfectly illustrates the effect of the hole concentration on the formation of LID defects. In fact, for n-type silicon sample, the majority carriers are electrons, and the excess minority carrier ‘holes’ are located only in the vicinity of light excitation.

	$P_{0= [B]-[P]}$ (10^{17} cm^{-3})	Local LID defect density (μs^{-1})	LID-spot (mm)	Diffused LID defect density (μs^{-1})
Sample A	1.2	1.7	4.8	0.2
Sample B	1.15	0.7	4	0.04
Sample E	-1.2	0.037	1.5	0.007

Table 2 LID defects characteristics

4. Conclusion

We have studied the local activation of light-induced degradation (LID) defects on highly co-doped B-P silicon wafers. A mapping of the minority carrier lifetime before and after defects activation allows estimating the defect concentration around the excitation point. We found that the LID defect concentration follows a Gaussian distribution as the excitation laser source. LID defects were obtained on all regions of the silicon sample which exhibits their diffusion from the excitation point. Phosphor was found to reduce the activity of LID defect. It is worth noting that lasers are frequently used in the engineering of silicon-based devices and then could activate LID defects; in such a case de-activation treatments at low temperature should be considered to assure silicon device performance.

Acknowledgments

The authors would like to gratefully thank the Tunisian Ministry of Higher Education and Scientific Research, and The Japan International Cooperation Agency for the financial support.

Data Availability Statement

The data that support the findings of this study are available from the corresponding author upon reasonable request.

References

- [1] T. Ishii, A. Masuda, *Progress in Photovoltaics: Research and Applications* 25 (2017) 953-967.
- [2] H. Fischer, Investigation of photon and thermal changes in silicon solar cells, *Conference Record of the 10th IEEE Photovoltaic Specialists Conference*, 1973, 1973.
- [3] J. Knobloch, S. Glunz, D. Biro, W. Warta, E. Schaffer, W. Wettling, Solar cells with efficiencies above 21% processed from Czochralski grown silicon, *Conference Record of the Twenty Fifth IEEE Photovoltaic Specialists Conference-1996*, IEEE, 1996, pp. 405-408.
- [4] J. Schmidt, A.G. Aberle, R. Hezel, Investigation of carrier lifetime instabilities in Cz-grown silicon, *Conference Record of the Twenty Sixth IEEE Photovoltaic Specialists Conference-1997*, IEEE, 1997, pp. 13-18.
- [5] J. Schmidt, Light-induced degradation in crystalline silicon solar cells, *Solid State Phenomena*, vol 95, *Trans Tech Publ*, 2004, pp. 187-196.
- [6] H. Hashigami, M. Dhamrin, T. Saitoh, *Japanese Journal of Applied Physics Part 1-Regular Papers Brief Communications & Review Papers* 42 (2003) 2564-2568.
- [7] H. Hashigami, Y. Itakura, T. Saitoh, *Journal of applied physics* 93 (2003) 4240-4245.
- [8] K. Bothe, J. Schmidt, *Journal of Applied Physics* 99 (2006) 11.
- [9] J. Geilker, W. Kwapil, S. Rein, *Journal of applied physics* 109 (2011) 053718.
- [10] V.V. Voronkov, R. Falster, Light-induced boron-oxygen recombination centres in silicon: Understanding their formation and elimination, *Solid State Phenomena*, vol 205, *Trans Tech Publ*, 2014, pp. 3-14.
- [11] M. Xie, C.R. Ren, L.M. Fu, X.D. Qiu, X.G. Yu, D.R. Yang, *Frontiers in Energy* 11 (2017) 67-71.
- [12] J. Schmidt, K. Bothe, V.V. Voronkov, R. Falster, *Physica Status Solidi B-Basic Solid State Physics* 257 (2020).
- [13] M. Winter, S. Bordihn, R. Peibst, R. Brendel, J. Schmidt, *IEEE Journal of Photovoltaics* 10 (2020) 423-430.
- [14] Z. Yao, D. Zhang, J. Wu, F. Jiang, G. Xing, X. Su, *Solar Energy Materials and Solar Cells* 218 (2020) 110735.
- [15] J. Adey, R. Jones, D. Palmer, P. Briddon, S. Öberg, *Physical review letters* 93 (2004) 055504.
- [16] H.W.B. V. G. Weizer, J. D. Broder, R. E. Hart, and J. H. Lamneck, *Photondegradation effects in terrestrial silicon solar cells*.
- [17] J. Corbett, A. Jaworowski, R. Kleinhenz, C. Pierce, N. Wilsey, *Solar cells* 2 (1980) 11-22.
- [18] S. Glunz, S. Rein, J. Lee, W. Warta, *Journal of Applied Physics* 90 (2001) 2397-2404.
- [19] J. Schmidt, A. Cuevas, *Journal of Applied Physics* 86 (1999) 3175-3180.
- [20] K. Bothe, J. Schmidt, *Applied Physics Letters* 87 (2005) 3.
- [21] K. Bothe, R. Hezel, J. Schmidt, *Applied physics letters* 83 (2003) 1125-1127.
- [22] A. Graf, A. Herguth, G. Hahn, *Aip Advances* 8 (2018) 7.
- [23] D. Macdonald, F. Rougieux, A. Cuevas, B. Lim, J. Schmidt, M. Di Sabatino, L. Geerligs, *Journal of Applied Physics* 105 (2009) 093704.
- [24] V.V. Voronkov, R. Falster, *Journal of Applied Physics* 107 (2010) 053509.
- [25] V. Voronkov, R. Falster, *physica status solidi (b)* 253 (2016) 1721-1728.
- [26] S. Dubois, N. Enjalbert, J. Garandet, *Applied Physics Letters* 93 (2008) 032114.
- [27] B. Lim, F. Rougieux, D. Macdonald, K. Bothe, J. Schmidt, *Journal of Applied Physics* 108 (2010) 103722.
- [28] Z. Liu, T. Carlberg, *Journal of The Electrochemical Society* 140 (1993) 2052.
- [29] H. Kodera, *Japanese journal of applied physics* 2 (1963) 212.
- [30] B.D. Rezgui, J. Veirman, S. Dubois, O. Palais, *physica status solidi (a)* 209 (2012) 1917-1920.
- [31] J. Veirman, S. Dubois, N. Enjalbert, J.-P. Garandet, M. Lemiti, *Journal of Applied Physics* 109 (2011) 103711.
- [32] J. Schmidt, K. Bothe, *Physical review B* 69 (2004) 024107.
- [33] D.K. Schroder, *IEEE transactions on Electron Devices* 44 (1997) 160-170.
- [34] W. Shockley, W.T. Read, *Physical Review* 87 (1952) 835-842.

- [35] G.L. Pearson, J. Bardeen, *Physical Review* 75 (1949) 865.
- [36] P. Altermatt, A. Schenk, G. Heiser, *Journal of Applied Physics* 100 (2006) 113715.
- [37] D.W. Palmer, K. Bothe, J. Schmidt, *Physical Review B* 76 (2007) 035210.